



Association of radiation belt electron enhancements with earthward penetration of Pc5 ULF waves: a case study of intense 2001 magnetic storms

M. Georgiou^{1,2}, I. A. Daglis¹, E. Zesta³, G. Balasis², I. R. Mann⁴, C. Katsavrias¹, and K. Tsinganos^{1,2}

¹Department of Physics, University of Athens, Panepistimiopoli Zografou, Athens, 15784, Greece

²Institute of Astronomy, Astrophysics, Space Applications and Remote Sensing, National Observatory of Athens, Vas. Pavlou & I. Metaxa, Penteli, 15236, Greece

³Goddard Space Flight Center, National Aeronautics and Space Administration, 8800 Greenbelt Rd, Greenbelt, MD 20771, USA

⁴Department of Physics, University of Alberta, Edmonton, Alberta, T6G 2E1, Canada

Correspondence to: M. Georgiou (margeo@phys.uoa.gr)

Received: 30 May 2015 – Revised: 12 October 2015 – Accepted: 18 October 2015 – Published: 20 November 2015

Abstract. Geospace magnetic storms, driven by the solar wind, are associated with increases or decreases in the fluxes of relativistic electrons in the outer radiation belt. We examine the response of relativistic electrons to four intense magnetic storms, during which the minimum of the Dst index ranged from -105 to -387 nT, and compare these with concurrent observations of ultra-low-frequency (ULF) waves from the trans-Scandinavian IMAGE magnetometer network and stations from multiple magnetometer arrays available through the worldwide SuperMAG collaboration. The latitudinal and global distribution of Pc5 wave power is examined to determine how deep into the magnetosphere these waves penetrate. We then investigate the role of Pc5 wave activity deep in the magnetosphere in enhancements of radiation belt electrons population observed in the recovery phase of the magnetic storms. We show that, during magnetic storms characterized by increased post-storm electron fluxes as compared to their pre-storm values, the earthward shift of peak and inner boundary of the outer electron radiation belt follows the Pc5 wave activity, reaching L shells as low as 3–4. In contrast, the one magnetic storm characterized by irreversible loss of electrons was related to limited Pc5 wave activity that was not intensified at low L shells. These observations demonstrate that enhanced Pc5 ULF wave activity penetrating deep into the magnetosphere during the main and recovery phase of magnetic storms can, for the cases examined, distinguish storms that resulted in increases in relativistic

electron fluxes in the outer radiation belts from those that did not.

Keywords. Magnetospheric physics (plasmasphere; storms and substorms) – space plasma physics (wave–particle interactions)

1 Introduction

Over the past decades, it has been well established that a geospace magnetic storm is the consequence of a chain of events originating from the Sun, evolving into a geoeffective solar wind flow before they ultimately reach the near-Earth space environment. Geospace magnetic storms are associated with either coronal mass ejections (CMEs) or high-speed solar streams (Gonzalez et al., 2007). Nonetheless, major magnetic storms have been found to be mainly caused by CMEs (Zhang et al., 2007), and these involve acceleration of charged particles in the Earth's radiation belts and intensification of electric current systems with characteristic signatures on the geomagnetic field (Daglis et al., 1999; Daglis, 2004).

Periodic oscillations in the Earth's magnetic field with frequencies in the range of a few millihertz (ultra-low-frequency (ULF) waves) can significantly influence radiation belt dynamics (Baker and Daglis, 2007) due to their potential for

strong interactions with charged particle populations. They can be driven by low-frequency mirror and drift instabilities of ring current ion populations (Ge et al., 2011). Anisotropy in the perpendicular ring current has also been proposed as a source of ULF wave growth (Takahashi et al., 1985). On the other hand, ULF waves can be generated externally by periodic variations in the solar wind dynamic pressure or variations in the orientation and strength of the interplanetary magnetic field (Hartinger et al., 2013). A different driver for the generation of such ULF waves is related to velocity shear between plasmas from different regions, such as the magnetosheath flow and the flowing solar wind along the magnetopause unstable to the Kelvin–Helmholtz instability (Claudepierre et al., 2008).

Furthermore, during periods of intensified geomagnetic activity, relativistic electron fluxes in the outer zone of the radiation belts exhibit substantial variation. Immediately after sudden commencement of magnetic storms, enhancements of relativistic electron fluxes have been observed on timescales of a few minutes (Kress et al., 2007). Relativistic electron flux variations are observed within longer timescales of up to days during the main and recovery phase of magnetic storms. The so-called “Dst effect”, describing the electron flux dropouts and subsequent increases in the recovery phase to levels exceeding the pre-storm ones due to large-scale changes in the geomagnetic field during storms (Turner et al., 2012), cannot explain variations on all different timescales.

The solar wind velocity and density fluctuations together with the north–south component of the interplanetary magnetic field (IMF) have been used to predict, by means of a model based on radial diffusion, some of the variability observed in relativistic electron fluxes during magnetic storms (Li, 2004). As the solar wind does not come in direct contact with the relativistic electrons in the outer radiation belt, radial diffusion, a result of drift-resonant interactions between relativistic electrons and Pc5 waves, was proposed for transporting electrons across their drift shells and accelerating them (Schulz and Lanzerotti, 1974). Radial diffusion requires a population of seed electrons of a few hundred kiloelectron volts which are supplied by substorms and subsequently energized by Pc5 waves. Depending on the general particle distribution, radial diffusion may act to increase electron flux levels in the inner magnetosphere as electrons diffuse earthward, breaking the drift invariant, Φ , while maintaining the gyro invariant, μ , and bounce invariant, J , associated with the trapped particles’ motion (Ukhorskiy et al., 2009; Ozeke et al., 2012, 2014). Radial diffusion may also act as a loss process as the aggregate of particles drift outward and are lost to the magnetopause (Turner et al., 2012).

Not surprisingly, while magnetic storms are often associated with enhancements of the electron flux in the outer radiation belts, they can also result in net depletions (Reeves et al., 2003). O’Brien et al. (2001a) identified conditions in the solar wind and the magnetosphere that lead to electron build-ups and dropouts. Specifically, enhanced Pc5 wave activity

during the recovery phase of magnetic storms appeared to differentiate best those storms that produce relativistic electrons along the geosynchronous orbit. Nonetheless, observations of increases or decreases in relativistic electron fluxes by satellites at a given orbit may not correspond to actual flux enhancement or electron losses throughout the outer radiation belt but rather be the results of an adiabatic modification of the drift paths of electrons. The comprehensive radiation belt observations from the Solar, Anomalous and Magnetospheric Particle Explorer (SAMPEX) allowed the study of long-term variations in relativistic electrons over a broad range of L shells. The radial profile of relativistic electron fluxes during the recovery phase of intense and moderate magnetic storms was found to be strongly dependent on solar wind parameters as well as the minimum value of the Dst index (Zhao and Li, 2013). In some extreme cases, powerful injections of electrons were observed in the slot region that is mostly devoid of energetic particles.

The study presented in this paper extends the results of previous investigations by focusing on selected magnetic storms during which ULF wave activity penetrated deep into the inner magnetosphere and examining their potential impact on relativistic electron penetration to low L shells (cf. a similar study by Loto’aniu et al., 2006, for the Halloween 2003 superstorm). We explore the variations in Pc5 wave power in both time and space for two distinct types of magnetic storms that include the magnetic storms that occurred in March and April 2001, when relativistic electron flux enhancements were observed in the recovery phase and the magnetic storm in August 2001 that exhibited a prolonged decrease in relativistic electron fluxes without subsequent recovery. Furthermore, since the inner edge of the outer electron radiation zone corresponds to the plasmopause location when this gets forced inwards during periods of intense geomagnetic activity (Goldstein et al., 2005; Li et al., 2006), we investigate how the plasmopause erosion favours migration of very energetic electrons in the slot region as well as penetration of Pc5 waves to low L shells.

2 Data sets and their analysis

We focus on four intense geospace magnetic storms that occurred during 2001, a period within the main phase of solar cycle 23. As a measure of storm intensity, we use the 1 h resolution final Dst index, provided by the World Data Center (WDC) for Geomagnetism of the Kyoto University, which was lower than -100 nT. A similar threshold for intense storms has been used by other authors as well (Gonzalez et al., 2007; Zhang et al., 2007). These were not preceded by any other magnetic storm within a period of 3 days before the Dst reached its minimum value and were not followed by any magnetic storm in the next 5 days.

We use measurements of relativistic electron fluxes from the energetic particle sensor EP8 onboard NOAA’s Geo-

stationary Operational Environmental Satellites (GOES) (Onsager et al., 1996), available on SPDF Coordinated Data Analysis Web (CDAWeb), to investigate the radiation belt electron flux level. The energetic particle sensor EP8 measures the directional, integral flux of electrons at energies greater than 2 MeV. The data used in this study have 5 min resolution. GOES-10 and GOES-8 orbited Earth at a geocentric distance of $6.6 R_E$, measuring electrons of relatively large pitch angles on a drift shell that corresponds to L^* shell approximately equal to 7 at midnight and close to 5 at noon – and even lower during intense magnetic storms. Using the statistical asynchronous regression (SAR), a method proposed to determine the relationship between two quantities without simultaneous measurements (O’ Brien et al., 2001b), the electron flux measurements have been reconstructed to local noon in order to distinguish temporal variations from the consequences of the orbital motion of the satellites.

Additional measurements of the radiation belts’ electron population covering the energy range between 2 and 6 MeV used in this study were collected by the Proton/Electron Telescope (PET) instrument on board the SAMPEX satellite (Cook et al., 1993). The near-polar orbit of SAMPEX had an altitude of approximately 600 km and a period of 96 min, allowing for completion of a full orbit around Earth 15 times each day and gathering of comprehensive measurements of both the inner and outer radiation belts. The satellite crosses the outer radiation belt at relatively high magnetic latitude, near the loss cone. Therefore, mostly energetic electrons of large equatorial pitch angle were observed (Li et al., 1997). The data collected have been averaged and sorted by L shell. If there were more than one electron flux measurement at an L -shell value, the average was calculated. For missing data at a particular L shell, nearest-neighbour interpolation was used to complete the radial profile of electron fluxes for L shells ranging from 1 to 10 with a spatial resolution of 0.1.

The temporal and spatial evolution of Pc5 wave activity during the four isolated magnetic storms was examined based on magnetic field measurements from ground-based magnetometer station arrays. These include time series of vector magnetic field measurements from the International Monitor for Auroral Geomagnetic effects (IMAGE) network covering L shells ranging from 3.29 to 15.43 in Scandinavia (Tanskanen, 2009) and stations from the magnetometer arrays providing data to the SuperMAG collaboration (Gjerloev, 2009), with more than 180 magnetic stations providing data for the period of interest in 2001. Figure 1 shows all magnetometer station locations used in this study, while the corrected geomagnetic coordinates (CGM), L shell, and magnetic local time (MLT) of noon in universal time (UT) of those stations located between 51.87 and 114.65° CGM longitudes are summarized in Table 1. For consistency with the magnetic coordinates provided for SAMPEX electron flux measurements, the International Geomagnetic Reference Field (IGRF) model has been used in their calcula-

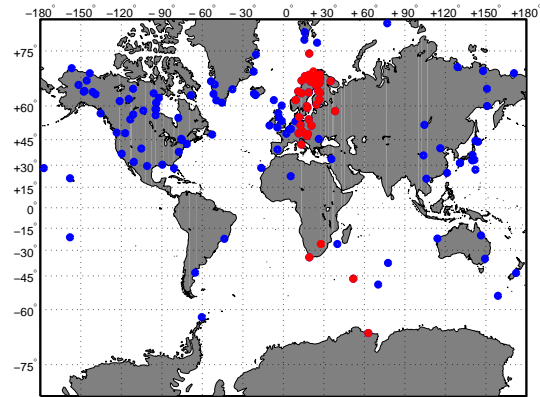


Figure 1. The geographic location of the magnetic stations from the IMAGE array and those contributing to SuperMAG archives from which magnetic field measurements were derived in this study. Specifically, measurements from the magnetic stations comprising the IMAGE array and magnetic stations at approximately the same geographic longitude, all highlighted in red, have been used in Figs. 3, 4, 6 and 7. In Figs. 5 and 8, magnetic field data from all magnetometers have been used.

tion and the L -shell value employed is the McIlwain L . The geomagnetic field measurements from IMAGE and SuperMAG magnetic stations have a temporal resolution of 10 s and 1 min, respectively. A continuous wavelet transform with the Morlet wavelet as the basis function has been applied to analyse them in the time–frequency domain. Prior to the time–frequency analysis using wavelet transforms, a sixth-order high-pass Butterworth filter with a cut-off frequency of 0.9 mHz was applied to obtain the wavelet power spectra covering the Pc4–5 frequency range (typically between 1 and 22 mHz) (Balasis et al., 2012, 2013).

3 Observations

3.1 Case studies of the March and April 2001 magnetic storms

Figure 2 shows hourly averaged electron fluxes with energy greater than 2 MeV measured by the GOES-10 satellite and daily averaged electron fluxes with energies between 2 and 6 MeV by SAMPEX as a function of L shell and time. Data cover the period from 1 January to 30 September 2001. Two intense magnetic storms that occurred in March 2001 were characterized by successively decreasing minima of the Dst index, which were equal to -140 and -387 nT. During the storm that followed on 12 April 2001, the Dst index reached a minimum value of -271 nT.

For each of these storms, we estimated the maximum electron flux as measured by the GOES-10 satellite over a period of 3 days prior to and 5 days after the Dst minima. We then calculated the ratio of the pre-storm to post-storm maximum electron flux. Their ratio was found to be greater than a fac-

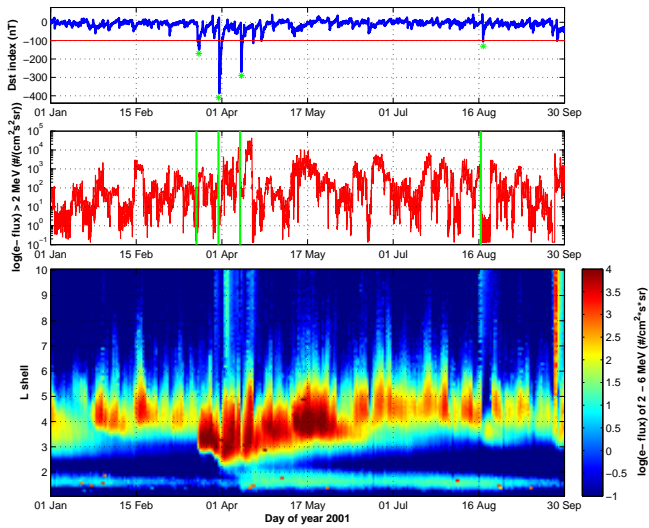


Figure 2. The period from 1 January to 30 September 2001 during solar cycle 23, when the four intense magnetic storms that this study is focused on occurred. From top to bottom, the hourly Dst index, hourly averaged electron measurements from the GOES-10 satellite, and daily averaged measurements of electrons with energies between 2 and 6 MeV from the SAMPEX satellite are shown. In the Dst index panel, the green asterisks are marks of the index minimum and the vertical lines in the GOES-10 observations panel indicate the commencements of the four intense magnetic storms that this study is focused on.

tor of 2 (see Table 2), a criterion also applied by Reeves et al. (2003) to define an electron flux change at geosynchronous orbit as an increase. In other words, these three magnetic storms are typical of magnetospheric events leading to a brief decrease in the relativistic electron fluxes observed in association with the build-up of the ring current and followed by a rapid increase during the recovery phase at geosynchronous orbit as well as in a broad range of *L* shells.

Furthermore, the *L*-shell location of the maximum electron flux and electrons’ deepest penetration in the slot region (*L* shells between roughly 2 and 3) was closely associated with the minimum value that the Dst index reaches in the main phase of each magnetic storm. Specifically, the most intense magnetic storm, on 31 March 2001, was characterized by the deepest injection of relativistic electrons to $L \approx 2 : 5$, while the peak of the electron fluxes was observed slightly below *L* shell = 3. The occurrence of the third consecutive magnetic storms on 12 April 2001 coincided with an enhancement of the inner radiation belt, which did not show significant variability during the previous two storms. However, we do not investigate the short-term variability in the inner radiation belt in this study.

The interplanetary driver of the main phase of each storm did not differ significantly among the three magnetic storms of March and April 2001 (see Zhang et al., 2007, for details). The solar wind structure associated with the intense and sus-

Table 1. Ground-based magnetometer locations.

Station	CGM lat (°)	CGM long (°)	<i>L</i> shell	UT (at noon MTL)
Northern Hemisphere				
BJN	71.89	107.71	9.89	09:02
SOR	67.80	106.04	6.75	09:09
TRO	67.07	102.77	6.37	09:22
AND	66.86	100.22	6.27	09:33
KEV	66.82	109.22	6.21	08:56
MAS	66.65	106.36	6.14	09:08
KIL	66.33	103.74	5.99	09:19
LEK	65.79	97.39	5.78	09:45
ABK	65.74	101.70	5.73	09:27
IVA	65.60	108.61	5.65	08:59
MUO	65.19	105.23	5.49	09:13
KIR	65.14	102.62	5.48	09:23
LOZ	64.77	114.65	5.30	08:35
SOD	64.41	107.33	5.18	09:04
PEL	64.03	104.97	5.05	09:13
RVK	62.61	93.27	4.61	09:03
OUL	62.11	105.42	4.44	09:11
NOR	61.87	94.84	4.39	09:56
LYC	61.87	99.33	4.38	09:37
OUJ	61.47	106.27	4.26	09:08
DOB	59.64	90.19	3.84	10:16
HAN	59.17	104.78	3.71	09:14
NUR	57.32	102.35	3.36	09:24
UPS	56.88	95.95	3.29	09:50
KVI	56.44	96.02	3.21	09:50
LOV	56.27	96.13	3.19	09:50
BOR	54.54	113.62	2.91	08:41
BFE	52.27	89.56	2.64	10:17
HLP	50.93	95.32	2.49	09:53
NGK	48.03	89.28	2.23	10:18
BEL	47.71	96.27	2.20	09:49
BDV	44.35	89.64	1.96	10:16
FUR	43.20	87.05	1.89	10:27
HRB	42.92	93.03	1.87	10:02
NCK	42.60	91.68	1.85	10:07
THY	41.72	92.25	1.80	10:05
AQU	35.74	87.68	1.54	10:24
Southern Hemisphere				
HBK	-35.51	96.36	1.53	23:13
HER	-42.08	84.09	1.83	23:47
CZT	-46.43	51.87	2.79	22:05
MAW	-67.61	62.88	8.77	22:41

tained geomagnetic activity was in three well-separated interplanetary coronal mass ejections (ICMEs) with a sheath of shocked plasma (SH) upstream. In Table 2 summarizing the main parameters of the interplanetary source of the magnetic storms studied, the ICME leading to the storms on 20 March and 12 April is referred to as magnetic cloud (MC). In these cases, the magnetic fields within the ICME were enhanced and their direction rotated (Klein and Burlaga, 1982).

The magnetosphere’s response reflected the increase observed in the solar wind speed and density as well as the

Table 2. Main parameters of the four selected magnetic storms in 2001.

Date, time	Min Dst (nT)	Solar wind structure	$V_{sw,max}$ ($km\ s^{-1}$)	IMF B_z,min (nT)	e -flux ratio	Max ULF power ($nT^2\ Hz^{-1}$)	$L\ shell_{ULF}$
20 March, 14:00	−149	SH+MC	525.38	−15.04	8.6667	614.5	6.75
31 March, 09:00	−387	SH+ICME	850.88	−53.82	10.3290	4.344	4.38
12 April, 00:00	−271	SH+MC	844.82	−35.84	2.2877	1.171	3.70
17 August, 22:00	−104	SH+MC	612.06	−21.96	0.0075	270.02	6.37

southward turning of the IMF. Specifically, the occurrence of the most intense magnetic storm on 31 March 2001 was associated with an extended interval of predominantly southward magnetic field (from 00:20 to 08:00 UT and from 12:50 UT on 31 March 2001 to 07:50 UT on 1 April 2001), where the IMF B_z component reached a minimum value of $-49\ nT$. The magnetopause was driven inside the geosynchronous orbit, while significant activity, including particle injection was observed in the magnetotail and duskward magnetosphere (Baker et al., 2002; Skoug et al., 2003). At the same time, the solar wind dynamic pressure (P_{dyn}) remained at levels as high as $58\ nPa$. Another such period of geomagnetic activity started on 11 April 2001 as a consequence of sustained southward IMF B_z component for approximately 10 h (with a minimum value of $-33\ nT$) and increased P_{dyn} (with a maximum value of $31\ nPa$) but of lower intensity.

Latitudinal Pc5 wave power distribution

To quantify the radial, in addition to the temporal, profile of ULF wave activity, we calculated a minatory index as the weighted sum of the wavelet power spectrum over Pc5 frequencies (between 1 and 10 mHz). We expect that our measure of the average Pc5 wave power includes substantial response to different forms of magnetospheric activity, such as storms and substorms, but it still provides a reliable proxy for ULF wave activity. For the production of the radial distribution of Pc5 wave power of the horizontal (x and y) component of the magnetic field, we used data from the IMAGE array and magnetic stations at lower magnetic latitudes that are located at magnetic longitudes between 84 and 114° (with the exception of two stations in the Southern Hemisphere included to extend the chain up to Antarctica). The magnetic coordinates of these 41 magnetic stations are summarized in Table 1.

During the course of each magnetic storm, prominent Pc5 waves were observed by the IMAGE network and magnetic stations located at CGM longitude around 100° , as evidenced by the mean wave power distribution. In the case of the magnetic storm on 31 March 2001 (see Fig. 3), power enhancements in this part of the wavelet power spectra were observed with the commencement of the magnetic storm at 04:00 UT (approximately 01:00 MLT) as well as during the next 3 days, before the Dst index recovered to its pre-

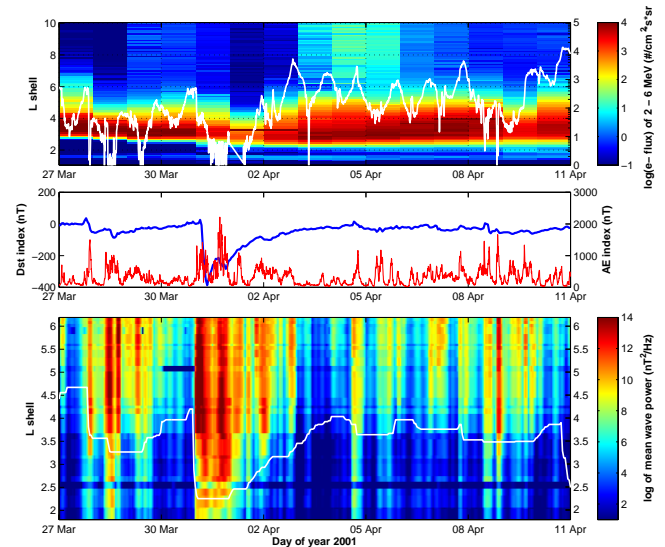


Figure 3. Mean Pc5 wave power (horizontal component) across the IMAGE network and magnetic stations located at approximately 110° CGM longitude from 27 March to 10 April 2001, an time interval when the magnetic storm of 31 March 2001 occurred. From top to bottom, daily averaged measurements of electrons with energies between 2 and 6 MeV from the SAMPEX satellite together with hourly averaged electron fluxes from the GOES-10 satellite, the Dst index together with the AE index, and the mean Pc5 wave power along with the plasmopause location are shown.

storm value. The intensity of Pc5 waves was strongly dependent on the phase of the magnetic storm during which they were observed. This latitudinal profile demonstrates that Pc5 wave activity was enhanced during the main phase of the magnetic storm and reached lower L shells as compared to the pre-storm period or after the recovery phase. The peak of Pc5 wave power was observed at $L\ shell = 4.38$ on 31 March 2001 (see Fig. 4 and Table 2) and 1 April (the main and early recovery phase of the storm) and moved to $L\ shell = 6.01$ on 2 April 2001.

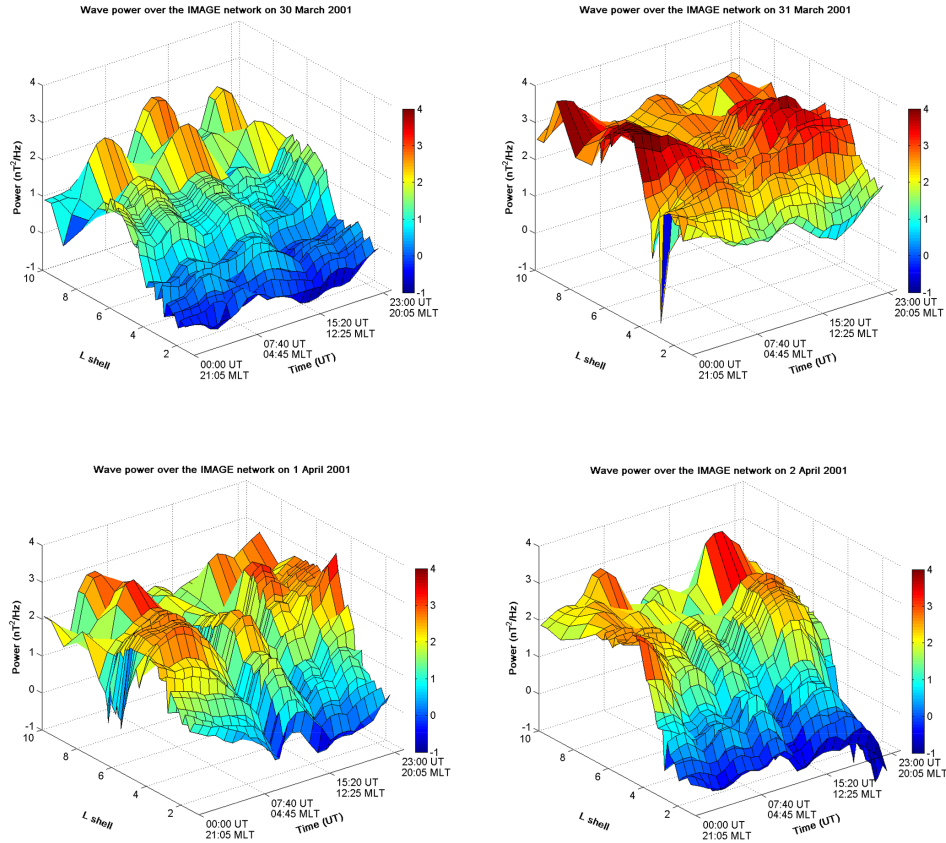


Figure 4. Daily distribution of mean Pc5 wave power (horizontal component) across the IMAGE network and magnetic stations located at approximately 110° corrected magnetic longitude during the 31 March 2001 magnetic storm. Each latitudinal profile covers L shells from 1.28 to 9.89, while the temporal resolution is 1 h.

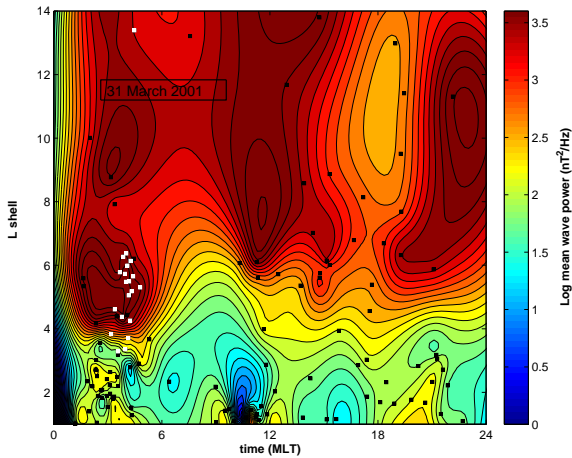


Figure 5. Mean Pc5 wave power (horizontal component) across a global network of magnetic stations, covering L shells from 1.02 to 13.80, during the main phase of the 31 March 2001 magnetic storm. The locations of each magnetic station are depicted as black squares, while IMAGE network stations are shown as white squares.

Global distribution of Pc5 wave power

For a more comprehensive picture of the spatial distribution of Pc5 wave power, we produced two-dimensional “snapshots” of our Pc5 wave index derived from all available measurements of the SuperMAG magnetic stations. In Fig. 5, the mean Pc5 wave power from a total of 131 magnetic stations is mapped in L shell vs. the MLT around which the stations were located in the time interval between 01:00 and 03:00 UT. The locations of the magnetic stations are shown with the black squares, while those of the IMAGE array are shown with white squares. Because of the uneven distribution of magnetic stations and the sparsity of measurements over extended regions of the Earth’s surface, the Pc5 wave power data have been interpolated on a constructed rectangular grid.

Figure 4 demonstrates that Pc5 wave activity was intensified on 31 March 2001, during the main phase of the magnetic storm. Moreover, Pc5 wave power was at high levels over all MLTs during the 2 h interval between 01:00 and 03:00 UT, as shown in Fig. 5. It should be noted that the Pc5 wave power distribution is asymmetric around local noon, concentrating around noon and the nightside (between

00:00 and 06:00 MLT and between 18:00 and 24:00 MLT), partially in agreement with the findings of past statistical surveys (Baker et al., 2003; Rae et al., 2012).

The Pc5 wave power peak was observed at L -shell values as low as 3.8 (see Fig. 4), which is comparable with the L -shell value where the peak electron flux is observed in SAMPEX measurements. We also found that the minimum plasmapause location, calculated by means of the empirical model developed by O'Brien and Moldwin (2003a), had then moved relatively close to Earth ($L_{p,\min} = 2.2$), inside the slot region. The plasmapause location was closely related to the inner boundary of the outer radiation belt, as Goldstein et al. (2005) demonstrated using SAMPEX measurements of 2–6 MeV electrons and extreme ultraviolet (EUV) images of the plasmasphere from the Imager for Magnetopause-to-Aurora Global Exploration. The rapid plasmasphere erosion and subsequent recovery was observed simultaneously with the evolution of the magnetic storm.

In other words, the unusual penetration of Pc5 waves during the main phase of the storm provided a means for their energization and intense substorm activity supplied electrons to fill the outer radiation belt in the recovery phase of the magnetic storm (Li et al., 2009). Relativistic electrons had the opportunity to occupy the slot region that would normally be inside the plasmasphere's outer boundary and also be accelerated just outside the high-plasma density plasmasphere. This behaviour is consistent with the findings of Loto'aniu et al. (2006), who demonstrated that ULF wave earthward penetration during the Halloween 2003 superstorm was observed together with the motion of the plasmapause towards a lower L shell. The ULF wave power was sufficiently strong to transport mega-electron-volt electrons to the low L -shell locations observed. Loto'aniu et al. (2006) attributed the penetration of the ULF waves to changes in the background plasma density due to O⁺ heavy ions upflowing from the ionosphere into the equatorial magnetosphere.

4 Control magnetic storm of August 2001

The response of the relativistic electrons in the outer radiation belt to the magnetic storm of 17 August 2001 was significantly different from the previous case studies, as Fig. 6 shows. Again, with the commencement of the storm, there was a rapid decrease in electron fluxes at geosynchronous orbit and L shells covered by the SAMPEX satellite, but the fluxes did not recover to their pre-storm levels before 22 August 2001 (that is, 6 days later). It should be noted that, during this magnetic storm, which is the least intense of the four storms studied, the decrease in electron fluxes was observed over L shells down to 3.5. This cannot be explained as a temporary, adiabatic dropout of electron fluxes, as the storm had recovered by 19 August, i.e. 3 days before the electron fluxes. Hence, the electron flux dropout should represent a true loss of particles due to irreversible (non-adiabatic) processes.

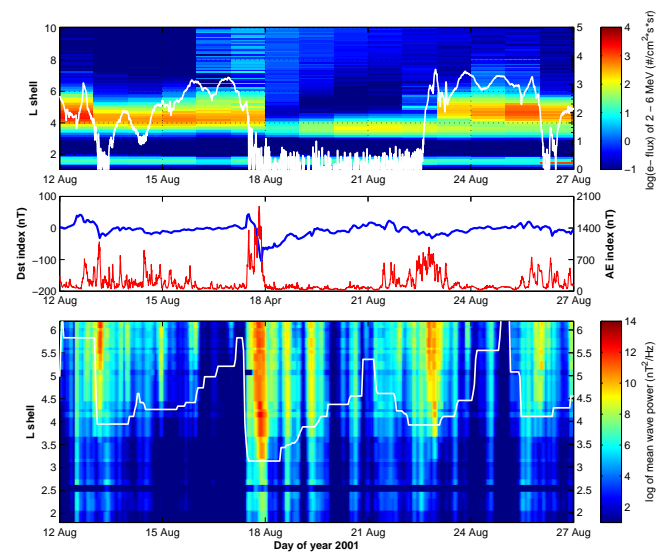


Figure 6. Mean Pc5 wave power (horizontal component) across the IMAGE network and magnetic stations located at approximately 110° CGM longitude together with geomagnetic activity indices and relativistic electron fluxes from 12 to 26 August 2001, a time interval when the magnetic storm of 17 August 2001 occurred.

On the basis of solar wind plasma and magnetic field signatures, the structure in the near-Earth solar wind leading to the magnetic storm of 17 August 2001 was identified as a magnetic cloud (see Zhang et al., 2007, for details), similar to the previous case studies. Nonetheless, a significantly shorter interval (from 15:00 to 19:50 UT) of southward IMF B_z reaching values as low as -22 nT depressed the Dst index to just below -100 nT. On the other hand, the solar wind flow pressure increase – expected to drive ULF waves in the magnetosphere – is significantly lower ($P_{\text{dyn,max}} \approx 28$ nPa) when compared to that of the ICME leading to the occurrence of the 31 March 2001 storm.

Latitudinal and global Pc5 wave distribution

Pc5 wave activity during the main phase of the magnetic storm of 17 August 2001, although sustained as shown in Fig. 6, was relatively low. Throughout the course of the storm, Pc5 wave power remained more than 1 order of magnitude lower than in the case of the 31 March 2001 magnetic storm. The increase was peaked further away from Earth, at L shell = 6.37. A second peak in Pc5 wave power is observed approximately 4 days after the commencement of the magnetic storm, on 22 August 2001. Nonetheless, enhanced Pc5 wave power close to Earth ($4 < L < 6$) (see Fig. 7), despite the global character seen in Fig. 8, is concentrated in the main phase of the storm.

This magnetospheric event serves as a control case for storms with sustained Pc5 wave activity during their main and recovery phase that produces relativistic electrons at

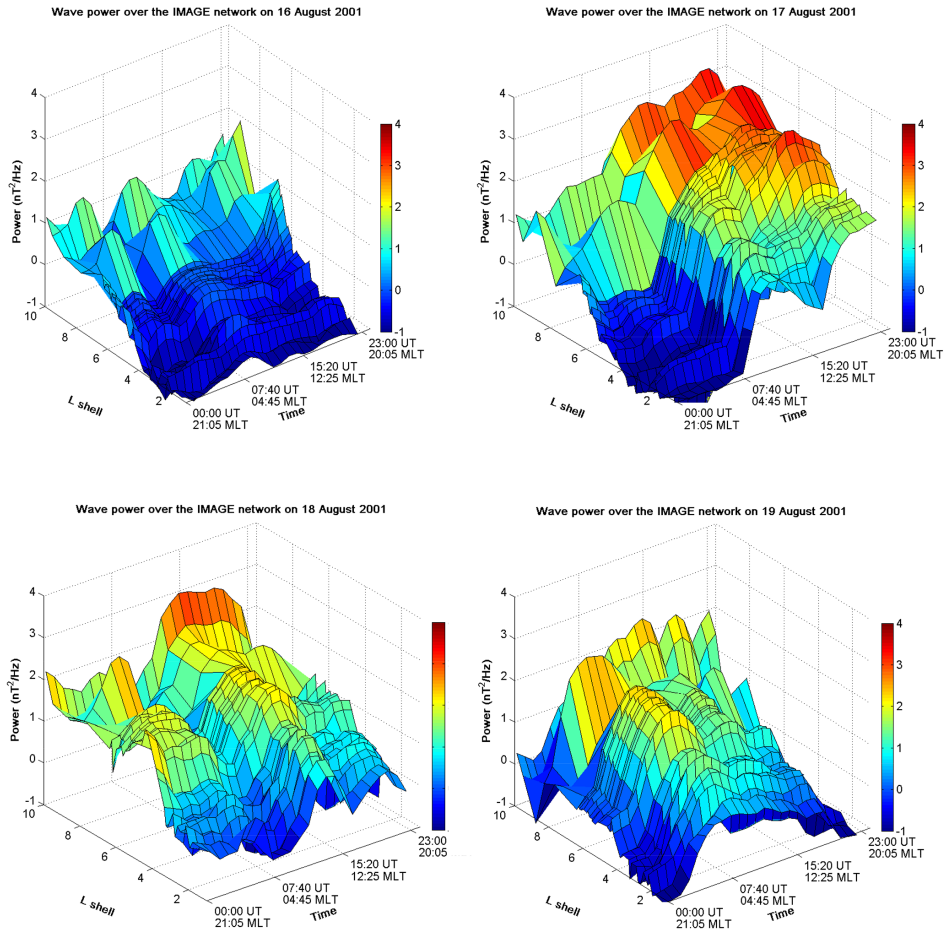


Figure 7. Daily distribution of mean Pc5 wave power (horizontal component) across the IMAGE network and magnetic stations located at approximately 110° corrected magnetic longitude during the 17 August 2001 magnetic storm.

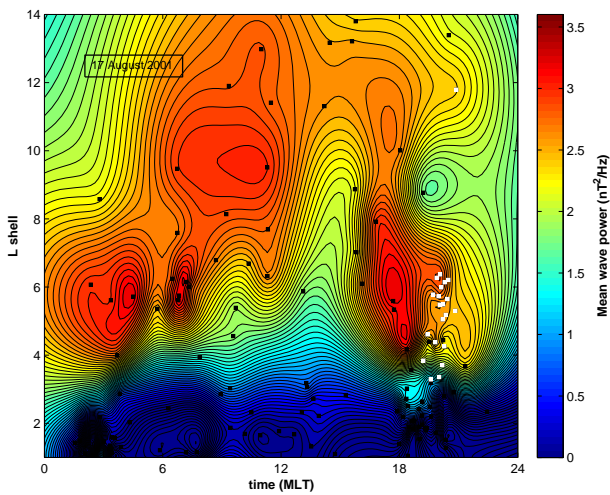


Figure 8. Mean Pc5 wave power (horizontal component) across a global network of magnetic stations, covering L shells from 1.02 to 13.80, during the main phase of the 17 August 2001 magnetic storm.

geosynchronous orbit as well as throughout the outer radiation belt. The magnetic storm of 17 August was of moderate intensity as the Dst index reached a minimum value of -104 nT and was accompanied by limited substorm activity. The conditions in the solar wind and the magnetosphere that drove the response of the outer radiation belt should be below the threshold for the erosion of the plasmasphere as well as the energization of the outer-belt electrons and their injection into the slot region.

5 Discussion and conclusions

Our study demonstrates a remarkable association between the earthward penetration of Pc5 waves and outer radiation belt electron enhancements during four selected magnetic storms that occurred in the 5-month period between 19 March and 22 August 2001. The increased fluxes of megaelectron-volt electrons measured during the recovery phase of these intense magnetic storms by GOES satellites at the geosynchronous orbit and the SAMPEX satellite across

the outer radiation belt were related to enhanced Pc5 wave activity throughout the storms. With the commencement of each storm, Pc5 wave activity built up and reached its peak during the main phase of the storm – almost simultaneously with the Dst minima. As the storm evolved, Pc5 wave activity penetrated deeper into the inner magnetosphere, ultimately reaching L shells as low as 2. The duration of enhanced wave activity depended on the strength of the magnetic storm and was sustained the longest during the most intense magnetic storm. It was also during the most intense storm of 31 March 2001 that the peak Pc5 wave power was observed the deepest into the magnetosphere, the same as the peak of the relativistic electron flux and the inner boundary of the outer electron radiation belt.

In the past, Pc5 waves had been observed at unusual depths in the inner magnetosphere during extreme magnetospheric events, such as the great magnetic storm of 24 March 1991 (Lee et al., 2007) and the magnetic super-storm of Halloween (Loto'aniu et al., 2006; Marin et al., 2014). This earthward penetration of ULF wave activity is not, however, limited to extreme magnetic storms. This was also observed during the relatively intense magnetic storms of March–April 2001, when it was able to play a key role in diffusing electrons radially inward and thereby accelerating them to higher energies. Recent calculations of radial diffusion coefficients over the L -shell range from 2.3 to 3.3 are consistent with this observational evidence. Specifically, Loto'aniu et al. (2006) calculated timescales of drift-resonant radial diffusion during the 2003 Halloween magnetic super-storm. They found them to be consistent with the timescales observed by SAMPEX for the increase in megaelectron-volt electron fluxes in the slot region.

We attribute the penetration of Pc5 wave activity down to the plasmasphere's outer boundary to the combined effects of externally and internally driven Pc5 waves. Specifically, strong southward IMF (B_z less than -15 nT), generated through the interaction between interplanetary disturbances (ICMEs and MCs) with the background solar wind and sustained for many hours (>5 h), has provided favourable conditions for the occurrence of intense magnetic storms (Daglis et al., 2003; Russell, 2007). During such intense magnetic storms, when the ring current is intensified, storm-time Pc5 waves are observed, closely linked to quasi-sinusoidal disturbances at Pc5 frequencies and injections of ring current ions in the inner magnetosphere (Barfield and McPherron, 1978). Storm-time Pc5 waves can reach radial distances of up to $L = 7.4$ (Barfield and Lin, 1983) and break the third adiabatic invariant through drift resonance with the outer radiation belt electrons to produce rapid radial transport even as low as $L = 4$ (Ukhorskiy et al., 2009).

On the other hand, the high solar wind dynamic pressure P_{dyn} (with a peak value greater than 15 nPa) that was observed during the passage of interplanetary shocks and CMEs should play a role in ULF wave growth through the Kelvin–Helmholtz instability at the magnetopause flanks (South-

wood, 1968) and compression of the dayside magnetopause (Kepko et al., 2002). The amplitude of externally driven waves rapidly declines with decreasing L shell (Vassiliadis et al., 2006; Rae et al., 2012), but, in concert with internally driven Pc5 waves, they can produce the enhanced wave activity observed in the heart of the outer radiation belt during the magnetic storms presented in this paper.

During the main phase of the intense magnetic storms of our study, the plasmasphere was severely eroded, with the plasmopause found inside the slot region (inside L shell ≈ 2) as previously calculated by Reinisch et al. (2004) and Goldstein et al. (2005). Given the enhanced Pc5 wave activity deep in the heart of the outer radiation belt, the severe erosion of the plasmasphere was followed by efficient local acceleration of electrons provided by sustained and intense substorm activity in the low-plasma-density region just outside the plasmasphere. We can conclude that enhanced Pc5 wave activity reaching L shells as low as 2 is an additional condition which, together with the plasmopause erosion and substorm activity, favours the enhancement of relativistic electrons in the recovery phase of intense magnetic storms and the transport of newly energized outer-belt electrons into the slot region. It remains to be seen whether the erosion of the plasmopause plays a causal role in enabling the penetration of ULF wave power to low L shells. As discussed by Loto'aniu et al. (2006), outside the depleted storm-time plasmopause, a region of enhanced heavy O^+ ions can develop in the form of a torus. It is this population of O^+ ions of ionospheric origin which changes the profile of the Alfvén continuum in the inner magnetosphere and enables the penetration of Pc5 wave power to much lower L shells than normal under these conditions.

Such enhanced Pc5 wave activity penetrating deep in the magnetosphere and its effects on particle motion are linked with radial diffusion (Ukhorskiy et al., 2009; Ozeke et al., 2012, 2014). Semi-periodic variations in magnetic and electric fields steering the drift motion of trapped electrons lead to particle diffusion across drift shells from regions of lower magnetic field strength to regions of increased magnetic field strength. Enhanced radial diffusion can result in electron acceleration and increases in radiation belt electron fluxes over timescales of hours. At the same time, microbursts – short bursts of precipitating relativistic electrons that are associated with whistler-mode chorus waves – were observed at equally small L shells (Johnston and Anderson, 2010), suggesting that electron flux peaks observed at L shells as low as approximately 3 might alternatively be related to dual ULF and VLF acceleration (O'Brien et al., 2003b; Reeves et al., 2013).

The observed radial profiles of Pc5 waves are characteristic of transport and acceleration of electrons from a source population located outside the radiation belts. During the most intense magnetic storms of March–April 2001, radial acceleration should have dominated over local acceleration

through chorus waves as these are accompanied by sustained substorm activity.

Acknowledgements. The work leading to this paper received funding from the European Union's Seventh Framework Programme (FP7-SPACE-2011-1) under grant agreement no. 284520 for the "Monitoring, Analyzing and Assessing Radiation Belt Energization and Loss" (MAARBLE) collaborative research project. This paper reflects only the authors views and the European Union is not liable for any use that may be made of the information contained herein. The publication costs are funded through the OpenAIRE project (Horizon 2020, grant agreement no. 643410). I. R. Mann is supported by a Discovery Grant from the Canadian NSERC.

For the ground magnetometer data used in this study, we gratefully acknowledge the following people and organizations: Intermagnet; USGS, J. J. Love; CARISMA, PI I. R. Mann; CANMOS; the S-RAMP database, PI K. Yumoto and K. Shiokawa; the SPIDR database; AARI, PI O. Troshichev; the MACCS programme, PI M. Engebretson, Geomagnetism Unit of the Geological Survey of Canada; GIMA; MEASURE, UCLA IGPP and Florida Institute of Technology; SAMBA, PI E. Zesta; 210 Chain, PI K. Yumoto; SAMNET, PI F. Honary; the institutes who maintain the IMAGE magnetometer array, PI E. Tanskanen; PENGUIN; AUTUMN, PI M. Connors; DTU Space, PI J. Matzka; South Pole and McMurdo Magnetometer, PIs L. J. Lanzarotti and A. T. Weatherwax; ICESTAR; RAPIDMAG; British Antarctic Survey; Mc-Mac, PI P. Chi; BGS, PI S. Macmillan; Pushkov Institute of Terrestrial Magnetism, Ionosphere and RadioWave Propagation (IZMIRAN); GFZ, PI J. Matzka; MFGI, PI B. Heilig; IGFPAS, PI J. Reda; University of L'Aquila, PI M. Vellante; ENIGMA, PI G. Balasis and I. A. Daglis, SuperMAG, PI J. W. Gjerloev. All ground magnetometer data can be accessed through the SuperMAG data service at <http://supermag.jhuapl.edu/>.

We also acknowledge the following sources of additional data: the Kyoto WDC for Geomagnetism and the observatories that produce and make AE and Dst indices available at <http://wdc.kugi.kyoto-u.ac.jp/>, SPDF CDAWeb and the science teams that provided interplanetary data through <http://cdaweb.gsfc.nasa.gov/>, NOAA's Space Environment Center at <http://www.ngdc.noaa.gov/stp/satellite/goes/>, and the Johns Hopkins University's Applied Physics Laboratory teams for energetic particle data available at <http://www.srl.caltech.edu/sampex/DataCenter/>.

The topical editor B. Mauk thanks C.-L.Huang and one anonymous referee for help in evaluating this paper.

References

Baker, D. N., Ergun, R. E., Burch, J. L., Jahn, J. -M., Daly, P. W., Friedel, R., Reeves, G. D., Fritz, T. A., and Mitchell, D. G.: A telescopic and microscopic view of a magnetospheric substorm on 31 March 2001, *Geophys. Res. Lett.*, 29, 1862, doi:10.1029/2001GL014491, 2002.

Baker, G. J., Donovan, E. F., and Jackel, B. J.: A comprehensive survey of auroral latitude Pc5 pulsation characteristics, *J. Geophys. Res.*, 108, 1384, doi:10.1029/2002JA009801, 2003.

Baker, D. N. and Daglis, I. A.: Radiation belts and ring current, in: *Space Weather – Physics and effects*, edited by: Bothmer, V. and Daglis, I. A., Springer Verlag, Berlin, Germany, 173–202, 2007.

Balasis, G., Daglis, I. A., Zesta, E., Papadimitriou, C., Georgiou, M., Haagmans, R., and Tsinganos, K.: ULF wave activity during the 2003 Halloween superstorm: multipoint observations from CHAMP, Cluster and Geotail missions, *Ann. Geophys.*, 30, 1751–1768, doi:10.5194/angeo-30-1751-2012, 2012.

Balasis, G., Daglis, I. A., Georgiou, M., Papadimitriou, C., and Haagmans, R.: Magnetospheric ULF wave studies in the frame of Swarm mission: A time-frequency analysis tool for automated detection of pulsations in magnetic and electric field observations, *Earth Planets Space*, 65, 1385–1398, doi:10.5047/eps.2013.10.003, 2013.

Barfield, J. N. and McPherron, R. L.: Stormtime Pc 5 magnetic pulsations observed at synchronous orbit and their correlation with the partial ring current, *J. Geophys. Res.*, 83, 739–743, 1978.

Barfield, J. N. and Lin, C. S.: Remote determination of the outer radial limit of stormtime Pc5 wave occurrence using geosynchronous satellites, *Geophys. Res. Lett.*, 10, 671–673, doi:0094-8276/83/003L-0881, 1983.

Claudepierre, S. G., Elkington, S. R., and Miltberger, M.: Solar wind driving of magnetospheric ULF waves: Pulsations driven by velocity shear at the magnetopause, *J. Geophys. Res.*, 113, A05218, doi:10.1029/2007JA012890, 2008.

Cook, W. R., Cummings, A. C., Cummings, J. R., Garrard, T. L., Kecman, B., Mewaldt, R. A., Selesnick, R. S., Stone, E. C., Baker, D. N., von Rosenvinge, T. T., Blake, J. B., and Callis, L. B.: PET: A proton/electron telescope for studies of magnetospheric, solar and galactic particles, *IEEE T. Geosci. Remote*, 31, 565–571, doi:10.1109/36.225523, 1993.

Daglis, I. A., Thorne, R. M., Baumjohann, W., and Orsini, S.: The terrestrial ring current: origin, formation and decay, *Rev. Geophys.*, 37, 407–438, doi:10.101029/1999RG900009, 1999.

Daglis, I. A., Kozyra, J. U., Kamide, Y., Vassiliadis, D., Sharma, A. S., Liemohn, M. W., Gonzalez, W. D., Trurutani, B. T., and Lu, D.: Intense space storms: Critical issues and open disputes, *J. Geophys. Res.*, 108, 1208, doi:10.1029/2002JA009722, 2003.

Daglis, I. A.: Geospace storm dynamics, in *Effects of Space Weather on Technology Infrastructure*, edited by: Daglis, I. A., Kluwer Academic Publishers, Dordrecht, 27–42, 2004.

Ge, Y. S., McFadden, J. P., Raeder, J., Angelopoulos, V., Larson, D., and Constantinescu, O. D.: Case studies of mirror-mode structures observed by THEMIS in the near-Earth tail during substorms, *J. Geophys. Res.*, 116, A01209, doi:10.1029/2010JA015546, 2011.

Gjerloev, J. W.: A global ground-based magnetometer initiative, *Eos*, 90, 230–231, doi:10.1029/2009EO270002, 2009.

Goldstein, J., Kanekal, S. G., Baker, D. N., and Sandel, B. R.: Dynamic relationship between the 350 outer radiation belt and the plasmopause during March–May 2001, *Geophys. Res. Lett.*, 32, L15104, doi:10.1029/2005GL023431, 2005.

Gonzalez, W. D., Echer, E., Clua-Gonzalez, A. L., and Tsurutani, B. T.: Interplanetary origin of intense geomagnetic storms ($Dst \leq -100$ nT) during solar cycle 23, *Geophys. Res. Lett.*, 34, L06101, doi:10.1029/2006GL028879, 2007.

Hartering, M. D., Turner, D. L., Plaschke, F., Angelopoulos, V., and Singer H.: The role of transient ion foreshock phenomena in driving Pc5 ULF wave activity, *J. Geophys. Res.*, 118, 299–312, doi:10.1029/2012JA018349, 2013.

- Johnston, W. R. and Anderson, P. C.: Storm time occurrence of relativistic electron microbursts in relation to the plasmopause, *J. Geophys. Res.*, 115, A02205, doi:10.1029/2009JA014328, 2010.
- Kepko, L., Spence, H. E., and Singer, H. J.: ULF waves in the solar wind as direct drivers of magnetospheric pulsations, *Geophys. Res. Lett.*, 29, 1197, doi:10.1029/2001GL014405, 2002.
- Klein, L. W. and Burlaga, L. F.: Interplanetary magnetic clouds at 1 AU, *J. Geophys. Res.*, 87, 613–624, 1982.
- Kress, B. T., Hudson, M. K., Looper, M. D., Albert, J., Lyon, J. G., and Goodrich, C. C.: Global MHD test particle simulations of >10 MeV radiation belt electrons during sudden storm commencement, *J. Geophys. Res.*, 112, A09215, doi:10.1029/2006JA012218, 2007.
- Lee, E. A., Mann, I. R., Loto'aniu, T. M., and Dent, Z. C.: Global Pc5 pulsations observed at unusually low L during the great magnetic storm of 25 March 1991, *J. Geophys. Res.*, 112, A05208, doi:10.1029/2006JA011872, 2007.
- Li, X., Baker, D. N., Temerin, M., Larson, D., Lin, R. P., Reeves, G. D., Looper, M., Kanekal, S. G., and Mewaldt, R. A.: Are energetic electrons in the solar wind the source of the outer radiation belt?, *Geophys. Res. Lett.*, 24, 923–926, doi:10.1029/97GL00543, 1997.
- Li, X.: Variations of 0.7–6.0 MeV electrons at geosynchronous orbit as a function of solar wind, *Adv. Space Res.*, 2, S03006, doi:10.1029/2003SW000017, 2004.
- Li, X., Baker, D. N., O'Brien, T. P., Xie, L., and Zong, Q. G.: Correlation between the inner edge of outer radiation belt electrons and the innermost plasmopause location, *Geophys. Res. Lett.*, 33, L14107, doi:10.1029/2006GL026294, 2006.
- Li, L. Y., Cao, J. B., Zhou, G. C., and Li, X.: Statistical roles of storms and substorms in changing the entire outer zone relativistic electron population, *J. Geophys. Res.*, 114, A12214, doi:10.1029/2009JA014333, 2009.
- Loto'aniu, T. M., Mann, I. R., Ozeke, L. G., Chan, A. A., Dent, Z. C., and Milling, D. K.: Radial diffusion of relativistic electrons into the radiation belt slot region during the 2003 Halloween geomagnetic storms, *J. Geophys. Res.*, 111, A04218, doi:10.1029/2005JA011355, 2006.
- Marin, J., Pilipenko, V., Kozyreva, O., Stepanova, M., Engebretson, M., Vega, P., and Zesta, E.: Global Pc5 pulsations during strong magnetic storms: excitation mechanisms and equatorward expansion, *Ann. Geophys.*, 32, 319–331, doi:10.5194/angeo-32-319-2014, 2014.
- O'Brien, T. P., McPherron, R. L., Sornette, D., Reeves, G. D., Friedel, R., and Singer, H. J.: Which magnetic storms produce relativistic electrons at geosynchronous orbit?, *J. Geophys. Res.*, 106, 15533–15544, doi:10.1029/2001JA000052, 2001a.
- O'Brien, T. P., Sornette, D., and McPherron, R. L.: Statistical asynchronous regression: Determining the relationship between two quantities that are not measured simultaneously, *J. Geophys. Res.*, 106, 13247–13259, doi:10.1029/2000JA900193, 2001b.
- O'Brien, T. P. and Moldwin, M. B.: Empirical plasmopause models from magnetic indices, *Geophys. Res. Lett.*, 30, 1152, doi:10.1029/2002GL016007, 2003a.
- O'Brien, T. P., Lorentzen, K. R., Mann, I. R., Meredith, N. P., Blake, J. B., Fennell, J. F., Looper, M. D., Milling, D. K., and Anderson, R. R.: Energization of relativistic electrons in the presence of ULF power and MeV microbursts: Evidence for dual ULF and VLF acceleration, *J. Geophys. Res.*, 108, 1329, doi:10.1029/2002JA009784, 2003b.
- Onsager, T., Grubb, R., Kunches, J., Matheson, L., Speich, D., Zwickl, R. W., and Sauer, H.: Operational uses of GOES energetic particle detectors, in *SPIE Proceedings 2812, GOES-8 and beyond*, edited by: Washwell, E. R., 281, doi:10.1117/12.254075, 1996.
- Ozeke, L. G., Mann, I. R., Murphy, K. R., Rae, I. J., Milling, D. K., Elkington, S. R., Chan, A. A., and Singer, H. J.: ULF wave derived radiation belt radial diffusion coefficients, *J. Geophys. Res.*, 117, A04222, doi:10.1029/2011JA017463, 2012.
- Ozeke, L. G., Mann, I. R., Murphy, K. R., Rae, I. J., and Milling, D. K.: Analytic expressions for ULF wave radiation belt radial diffusion coefficients, *J. Geophys. Res.*, 119, 1587–1605, doi:10.1002/2013JA019204, 2014.
- Rae, I. J., Mann, I. R., Murphy, K. R., Ozeke, L. G., Milling, D. K., Chan, A. A., Elkington, S. R., and Honary, F.: Ground-based magnetometer determination of in situ Pc4–5 ULF electric field wave spectra as a function of solar wind speed, *J. Geophys. Res.*, 117, A04221, doi:10.1029/2011JA017335, 2012.
- Reeves, G. D., McAdams, K. L., Friedel, R. H. W., and O'Brien, T. P.: Acceleration and loss of relativistic electrons during geomagnetic storms, *Geophys. Res. Lett.*, 30, 1529, doi:10.1029/2002GL016513, 2003.
- Reeves, G. D., Spence, H. E., Henderson, M. G., Morley, S. K., Friedel, R. H. W., Funsten, H. O., Baker, D. N., Kanekal, S. G., Blake, J. B., Fennell, J. F., Claudepierre, S. G., Thorne, R. M., Turner, D. L., Kletzing, C. A., Kurth, W. S., Larsen, B. A., and Niehof, J. T.: Electron acceleration in the heart of the Van Allen radiation belts, *Science*, 341, 991–994, doi:10.1126/science.1237743, 2013.
- Reinisch, B. W., Huang, X., Song, P., Green, J. L., Fung, S. F., Vasyliunas, V. M., Gallagher, D. L., and Sandel, B. R.: Plasmaspheric mass loss and refilling as a result of a magnetic storm, *J. Geophys. Res.*, 109, A01202, doi:10.1029/2003JA009948, 2004.
- Russell, C. T.: The coupling of the solar wind to the Earth's magnetosphere, in *Space weather – Physics and effects*, edited by: Bothmer, V. and Daglis, I. A., Springer Praxis Books, 103–130, 2007.
- Schulz, M. and Lanzerotti, L. J.: *Particle Diffusion in the Radiation Belts, Physics and chemistry in space*, 7, Springer, New York, doi:10.1007/978-3-642-65675-0, 1974.
- Skoug, R. M., Thomsen, M. F., Henderson, M. G., Funsten, H. O., Reeves, G. D., Pollock, C. J., Jahn, J. -M., McComas, D. J., Mitchell, D. G., Brandt, P. C., Sandel, B. R., Clauer, C. R., and Singer, H. J.: Tail-dominated storm main phase: 31 March 2001, *J. Geophys. Res.*, 108, 1259, doi:10.1029/2002JA009705, 2003.
- Southwood, D. J.: The hydromagnetic stability of the magnetopause boundary, *Planet. Space Sci.*, 16, 587–605, 1968.
- Takahashi, K., Russell, C. T., and Anderson, R. R.: ISEE 1 and 2 observations of the spatial structure of a compressional Pc5 wave, *Geophys. Res. Lett.*, 12, 613–616, doi:10.1029/GL012i009p00613, 1985.
- Tanskanen, E. I.: A comprehensive high-throughput analysis of substorms observed by IMAGE magnetometer network: Years 1993–2003 examined, *J. Geophys. Res.*, 114, A05204, doi:10.1029/2008JA013682, 2009.
- Turner, D. L., Shprits, Y., Hartinger, M., and Angelopoulos, V.: Explaining sudden losses of outer radiation belt elec-

- trons during geomagnetic storms, *Nat. Phys.*, 8, 2008–2012, doi:10.1038/nphys2185, 2012.
- Ukhorskiy, A. Y., Sitnov, M. I., Takahashi, K., and Anderson, B. J.: Radial transport of radiation belt electrons due to stormtime Pc5 waves, *Ann. Geophys.*, 27, 2173–2181, doi:10.5194/angeo-27-2173-2009, 2009.
- Vassiliadis, D., Mann, I. R., Fung, S. F., and Shao, X.: Ground Pc3–Pc5 wave power distribution and response to solar wind velocity time variations, *Planet. Space Sci.*, 55, 743–754, doi:10.1016/j.pss.2006.03.012, 2006.
- Zhang, J., Richardson, I. G., Webb, D. F., Gopalswamy, N., Huttunen, E., Kasper, J. C., Nitta, N. V., Poomvises, W., Thompson, B. J., Wu, C.-C., Yashiro, S., and Zhukov, A. N.: Solar and interplanetary sources of major geomagnetic storms ($Dst \leq 100nT$) during 1996–2005, *J. Geophys. Res.*, 112, A12103, doi:10.1029/2007JA012891, 2007.
- Zhao, H. and Li, X.: Inward shift of outer radiation belt electrons as a function of Dst index and the influence of the solar wind on electron injections into the slot region, *J. Geophys. Res.*, 118, 756–764, doi:10.1029/2012JA018179, 2013.